

Characterization of Goldstrike ore carbonaceous material

Part 1: Chemical characteristics

J.F. Stenebråten, W.P. Johnson and D.R. Brosnahan

Abstract

Carbonaceous materials (CM) from ores of varying preg-robbing activity from Barrick Goldstrike Mines Inc. (BGMI), Nevada, were characterized in terms of their functional group contents, hydrocarbon contents, elemental compositions and humic acid contents. Fourier transform infrared (FT-IR) analyses did not show the presence of hydrocarbons or carboxylic, phenolic or sulfhydryl functionalities. The FT-IR bands present included C=C stretching in aromatic rings and C-O-C stretching, indicating the presence of oxygen as ether linkages or thiocarbonyl functionality in the carbon matrix. Calculated atomic oxygen to carbon (O/C) ratios did not reveal a trend between the maturity of the CM and the preg-robbing behavior, possibly due to the low resolution inherent in electron microprobe analyses. However, the atomic O/C ratios agree with other chemical analyses, indicating that the organic carbon is very mature, similar to or higher than anthracite grade coal. Gas chromatography-mass spectrometry and nuclear magnetic resonance analyses corroborated the relatively featureless character of the carbon, indicating that the carbon structure is virtually completely aromatic (graphitic).

Key words: Ore characterization, Gold processing, Carbonaceous ore, Preg-robbing

Introduction

The characterization of the carbonaceous matter (CM) present in ore from the Barrick Goldstrike Mines, which is located within the Carlin trend in Nevada, was motivated by concern for its preg-robbing behavior. The term "preg-robbing" was first used by Smith (1968) and later by Hausen and Bucknam (1985) to describe poor recovery of gold during processing. Previous studies indicated that natural organic carbon in the ore is associated with the preg-robbing behavior. Hence, subsequent studies have attempted to deduce the characteristics of the organic carbon responsible for preg-robbing (Radtke and Scheiner, 1970; Hausen and Bucknam, 1985). Radtke and Scheiner (1970) reported the following three types of organic carbon in Carlin ore:

- carbon similar in nature to activated carbon,
- long-chain aliphatic hydrocarbons and
- humic acids.

The presence of aliphatic hydrocarbons and humic substances was not observed in subsequent studies (Nelson et al., 1982; Leventhal and Hofstra, 1990; Sibrell et al., 1990), and moieties previously thought to represent humic substances are now believed to be due to contamination from blast residues, such as ammonium nitrate and diesel fuel (Leventhal and Hofstra, 1990). The presence of hydrocarbons in carbonaceous matter from Carlin ores, although reported, does not appear to be a general attribute of Carlin carbonaceous ores. Nelson et al. (1982) used photoacoustic infrared spectroscopy and laser Raman spectroscopy to determine the presence of activated carbon type structures, but neither organic hydrocarbons nor humic acid materials were detected. Hausen and Park (1985), using hydrogen/carbon (H/C) ratios, infrared (IR) spectroscopy and vitrinite reflectance, reported the organic carbon in Carlin ore to be pyrobitumen with a high carbon content (up to 80%) and assigned a coal rank of the carbonaceous material of semianthracite to anthracite. Sibrell et al. (1990) used Fourier transform infrared (FT-IR) spectroscopy to characterize ore from the Carlin Mine and observed no humic substances or significant amounts of hydrocarbons. It was concluded that the organic material was mostly aromatic carbon with an activated carbon type structure, similar in maturity to anthracite-grade coal.

The present study was initiated to characterize the carbonaceous material in Goldstrike ore with respect to its possible humic or hydrocarbon content and to provide a basis for evaluating potential mechanisms of gold sorption. Sixteen samples from BGMI were studied. The samples had preg-robbing behavior ranging from low to high, as described in Stenebråten et al. (1998). The samples were obtained from various deposits at the BGMI property (e.g., Rodeo, Screamer, Betze and Meikle). The extreme variation in carbonaceous material concentration, as well as preg-robbing behavior observed from sample to sample within these deposits, obviates the need for further description of these deposits. Rather,

J.F. Stenebråten and W.P. Johnson are graduate student and assistant professor, respectively, with the Department of Geology and Geophysics, University of Utah, Salt Lake City, UT; D.R. Brosnahan, member SME, is chief mineralogist with Barrick Goldstrike Mines Inc., Elko, NV. Nonmeeting paper number 98-318. Original manuscript submitted for review March 1998. Revised paper accepted for publication December 1998. Discussion of this peer-reviewed and approved paper is invited and must be submitted to SME prior to Feb. 29, 2000.

the samples are referred to according to their measured preg-robbing behavior.

Because the carbonaceous matter in Carlin trend ores is described as being similar to activated carbon and anthracite coal, spectroscopic studies of activated carbon and coal are relevant to this study. IR spectroscopy has been used extensively by the coal industry to characterize coal functionality (Painter et al., 1981; Zerda et al., 1981; Snyder et al., 1983; Sobkowiak and Painter, 1992). One of the important controversies from this research concerns the prominent peak that is present at $1,582\text{ cm}^{-1}$. The peak is considered characteristic of C=C bond stretching in the hexagonal ring structure of graphite, which is the endpoint for thermal maturation (crystallization) of amorphous carbon (Mantell, 1968). Graphite is comprised of a hexagonal crystal structure, consisting of stacked planar layers of aromatic rings, with the layers held together by weak van der Waals forces. The shortest interatomic distance within the plane of a perfect hexagonal ring is 1.42 \AA , while the shortest distance perpendicular to the sheets of hexagonal rings is 3.349 \AA . With a loss of packing density due to incomplete graphitization, a loss in the three-dimensional crystallinity is observed (Tuinstra and Koenig, 1970).

The C=C bond should theoretically be IR-inactive in highly ordered structures such as graphite (Starsinic et al., 1983). This is because IR activity requires an asymmetric bond to result in a variation of the dipole moment across the bond (Skoog and West, 1980). However, the $1,582\text{ cm}^{-1}$ peak is observed in coal and activated carbon (Painter et al., 1983; Starsinic et al., 1983; Sibrell, 1991), and two possible explanations of the origin of C=C asymmetry exist. The first is derived from structural irregularities in the polymeric aromatic matrix (Painter et al., 1983; Starsinic et al., 1983). The second is due to the presence of polar functional groups, i.e., phenolic or carboxylic, attached to the aromatic rings (Painter et al., 1981; Snyder et al., 1983; Starsinic et al., 1983).

The objective of this paper is to characterize the functionality and elemental composition of the CM associated with gold ores of varying preg-robbing activities at BGMI. To the author's knowledge, there exists only one other study examining the properties of natural carbonaceous matter using the techniques reported here. This study serves as a basis for further examination of the properties of natural carbonaceous matter in BGMI ores, which will be the subject of Part 2 of this series (Stenebråten, Johnson and McMullen, to be published in a future issue of *Minerals & Metallurgical Processing*).

Methods

The analyses used in this study were FT-IR, electron microprobe, gas chromatography-mass spectrometry (GC-MS) and $\delta^{13}\text{C}$ nuclear magnetic resonance (CP/MAS-NMR) spectroscopy. Results of laser Raman spectroscopy, X-ray diffraction (XRD), surface area, micropore-size distribution analyses and the effects of ball mill grinding on the above physical characteristics will be reported in Part 2 of this series.

Demineralization procedure. It was necessary to remove silicates and carbonates originally in the Goldstrike ore, not only because of their interference in the XRD analysis for graphite, but also to enhance the resolution of spectroscopic analyses of the carbonaceous material. Silicates and carbonates were removed by acid digestion using hydrochloric acid (HCl), hydrofluoric acid (HF) and boric acid, according to the procedure of Tafuri (1987). The procedure involved saturation of 400 g of dried and pulverized ore

in 0.1 N HCl (1,000 mL). When the initial effervescence ceased, 5-mL aliquots of concentrated HCl were added until all carbonate minerals were digested and no further effervescence occurred. The slurry was then filtered through Whatman #1 filter paper, rinsed with distilled water and filtered again. While the residue was still damp, it was carefully moistened with concentrated HF. Care was exercised to avoid violent reaction of finely ground residue with HF, which would cause residue to spatter from the container. Upon thorough moistening with HF, the residue was slowly submerged in 400 mL of HF and placed on a shaker table to ensure complete acid-rock contact. Each HF bath lasted a minimum of three days, and three to five repetitions were required to obtain a silicate-free residue, which was verified by XRD, electron microprobe and FT-IR. At the end of each HF bath, the mixture was slurried with 800 mL of saturated boric acid to complex fluoride and to avoid the formation of insoluble fluoride salts. The mixture was filtered after reacting for 10 min. While the equilibration liquid was discarded, the solids were slurried in distilled water and filtered again. After each filtration step, the filter paper was rinsed and the filter cake returned to the sample.

Density separation. Following the acid-digestion demineralization procedure, the weight percent of organic carbon in the concentrate ranged from 2.46% to 41.10% (Table 1), as determined by LECO analyses performed by BGMI Metallurgical Services. The low preg-robbing samples (Samples #8 and #9) contained the least amount of carbonaceous material, with sulfides being the major noncarbonaceous contributor to those concentrates. The low percentage of carbonaceous material deteriorated the signal from XRD and spectroscopic analysis, and, hence, an increase of carbonaceous material concentration was desirable.

Density separation by sodium polytungstate (SPT) ($3\text{Na}_2\text{WO}_4 \cdot 9\text{WO}_3 \cdot \text{H}_2\text{O}$) from Sometu-US resulted in sufficient separation for this study. SPT is inert with respect to organic material (Sometu-US, personal communication). Thus, fractionation of CM due to interaction with the SPT would not be expected during this separation. SPT density was adjusted with water to 2.5 g/cm^3 to ensure separation of carbonaceous material ($\text{SG}_{\text{graphite}} = 2.23$) and bulk sulfides ($\text{SG}_{\text{pyrite}} = 5.02$). From observations with a petrographic microscope, sulfides remaining in the suspension after SPT separation occurred as inclusions in the carbonaceous matter and as minute free particles. The SPT separation procedure was performed on approximately 5 g of demineralized material, which was submerged in 25 mL of SPT in a 50-mL flask (Kimax) and blended by shaking. The centrifuge tube was then placed in a sonicator (Branson) for 20 min to disaggregate the sample, followed by centrifugation for 15 min. at 1,000 rpm (Beckman Avanti). The liquid was decanted and filtered through a 1.2-mm pore size acetate filter (MSI). The filter cake was resuspended and rinsed with deionized water to remove any remaining SPT, filtered and evaporated at 30°C until dry. SPT was not reused, to prevent possible contamination between samples. After density separation, the organic carbon content ranged from 11.34% to 83.60% (Table 1). Samples that underwent demineralization and density separation are referred to as CM in this report.

FT-IR. For the FT-IR analyses, the CM was diluted (1:50) with spectroscopic-grade KBr, and the mixture was ground for 5 min. using an agate mortar and pestle to homogenize the two components and to reduce potential scattering effects of

larger sample particles. A BioRad Digilab FTS 40 spectroscope and sample holder (Spectra Tech) was used for the diffuse reflectance FT-IR analyses. The atmosphere surrounding the sample was purged with N₂ to remove CO₂ and other gases that would otherwise contribute to the spectra.

Electron microprobe. Electron microprobe analyses were performed to determine the elemental composition of the CM and to study the maturity rank, which is inversely correlated to the atomic oxygen to carbon ratio (Leventhal, 1985). Silicon was included in the analyses to verify that the CM was free from silicates and, in cases where minute quantities of silicon persisted, to correct for any oxygen bound to this silicon. The electron beam was focused onto individual carbonaceous particles and care was taken to avoid other mineral inclusions (i.e., sulfides) present in the CM.

Samples were mounted in 25.4-mm- (1-in.-) diam. epoxy plugs by drilling holes through each plug and pouring a small amount of CM powder into the holes, of which one end had been covered with tape.

A few drops of thermal epoxy were stirred into each sample, and, after a homogeneous mix was reached, the remaining volume of the hole was filled with thermal epoxy. Thermal epoxy was required because ordinary two-component epoxy did not harden when mixed with the very fine-grained carbonaceous powder. The epoxy plugs were then exposed to a hotplate (~130°C) for approximately 10 min., which was sufficient to allow the thermal epoxy to harden. The plugs were then polished first using a 45- μ m and then a 15- μ m wet-diamond rotating polishing-plate. This was followed by a wet 1-mm alumina-powder rotating polishing-plate. For a final polish, the epoxy plugs were cleaned for six hours in a sonic cleaner and polished on a Syntron vibratory polisher in a 0- to 2- μ m diamond-paste bath. Before analysis, the plugs were carbon-coated to cover any insulating specimens with a conducting surface layer to prevent charging.

The samples were examined by a Cameca SX 50 electron microprobe with X-ray wavelength dispersive technique for the following elements: Si, As, Fe, Zn, S, O and C. A thallium acid phthalate (TAP) crystal was used for the analysis of silicon. A lithium fluoride (LiF) crystal was used for the analysis of arsenic, iron and zinc, whereas a pentaerythritol (PET) crystal was employed for the sulfur analysis. For analysis of the light elements, oxygen and carbon, a PC-1 crystal was used. The PC-1 is a synthetic multilayer crystal made of alternating layers of Si and W with a 2d spacing of 93.5 Ångströms. The large 2d spacing is required for analysis of light elements, due to their low critical excitation energy. The standards used for calibration of analyses were synthetic diamond for C, calcite for O, synthetic sphalerite for Zn, pyrite for Fe and S, arsenopyrite 57 for As and quartz for Si.

GC-MS. Pyrolysis Curie-point GC-MS was performed under inert conditions (ultrahigh purity He). Analyses were performed by the Center for Micro Analysis and Reaction Chemistry at the University of Utah. Demineralized carbon-

Table 1 — Leco results showing total and organic carbon percentages in ore after demineralization and after demineralization and float-sink procedure.

Sample I.D.	Before demineralization		After demineralization		After demineralization and float-sink	
	Total carbon, %	Organic carbon, %	Total carbon, %	Organic carbon, %	Total carbon, %	Organic carbon, %
# 1	2.80	1.10	30.44	30.14	44.02	44.02
# 2	1.00	1.00	14.78	14.78	26.05	26.10
# 3	4.60	3.70	41.10	41.10	52.52	52.52
# 4	2.10	0.60	11.72	11.68	20.98	20.98
# 5	1.60	1.20	21.96	21.96	36.41	36.41
# 6	5.20	0.40	17.62	17.62	30.48	30.48
# 7	3.10	2.10	32.53	32.53	40.97	40.97
HPR-1	5.90	4.40	N/K	N/K	83.60	83.60
0421	7.92	7.92	N/K	N/K	67.11	67.11
0418	8.31	8.31	N/K	N/K	68.96	68.96
0415	9.07	3.02	N/K	N/K	68.33	68.33
#11	4.90	1.00	N/K	N/K	53.78	53.78
LPR-1	3.80	3.20	N/K	N/K	64.64	64.64
#8	N/K	0.30	2.50	2.46	11.34	11.34
#9	N/A	0.20	4.85	4.85	13.32	13.32
0595	N/A	N/A	N/K	N/K	53.94	53.94

aceous material (0.5 mg) was suspended in hexane (5 mL) and agitated overnight to remove fatty acids potentially introduced during processing. The carbonaceous samples were suspended in methanol (5 mL). The bulk of the carbon settled out of suspension, while the finest particles remained in the supernatant. The supernatant and a blank methanol solution were submitted for GC-MS analysis. Samples were coated on pyrolytic wires (0.5-mm-diam) characterized by a Curie-point temperature of 610°C. Aliquots of the supernatant (5 μ L) were placed on the tips of the pyrolytic wires, and the solvent was allowed to evaporate at room temperature. Coated wires were withdrawn into borosilicate glass tubes and inserted into the Curie-point pyrolyzer. Chromatographic separation was performed using a fused silica capillary column (12-m x 0.25-mm i.d., coated with DB-5ms liquid phase, film thickness 0.25 μ m). Organic products were analyzed using a mass spectrometer (Finnigan-MAT Ion Trap Detector Model 700).

CP/MAS NMR. To further test for the presence of aliphatic hydrocarbons and oxygenated functional groups, the solid demineralized samples were analyzed by nuclear magnetic resonance (δ^{13} C CP/MAS NMR) spectroscopy. Ten thousand scans were taken of samples 0595, a low preg-robbing sample (LPR), and sample 0421, a high preg-robbing sample (HPR), while 56,000 scans were taken of sample 0418 (HPR). A line-broadening value of 25 was used for samples 0595 and 0421, and a value of 100 was used for sample 0418. Despite the slight differences in experimental conditions between the two HPR samples, their spectra were very similar, as will be described below. Pulse width varied from 4.20 to 6.0 μ s, and contact time varied from 5.0 to 3.0 μ s. A spectrum width of 20,000 kHz was employed for all samples with a spin cycle of 4.1 kHz. A brief description of the peak locations in NMR spectra from natural organic matter is listed in Table 2. Analyses were performed by the

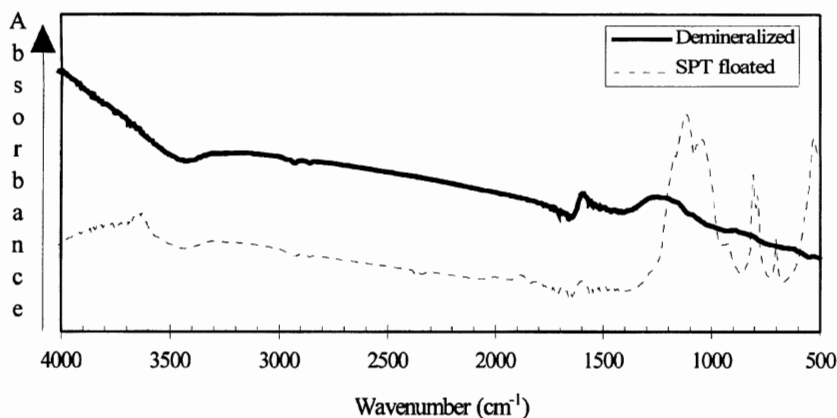


Figure 1 — Characteristic FT-IR scan showing a broad peak at $1,250\text{ cm}^{-1}$ and a C=C peak at $1,582\text{ cm}^{-1}$ observed for samples after acid digestion and SPT flotation (demineralized). An FT-IR scan of one sample after SPT flotation only (SPT-floated) shows, in comparison to the other sample, much poorer resolution.

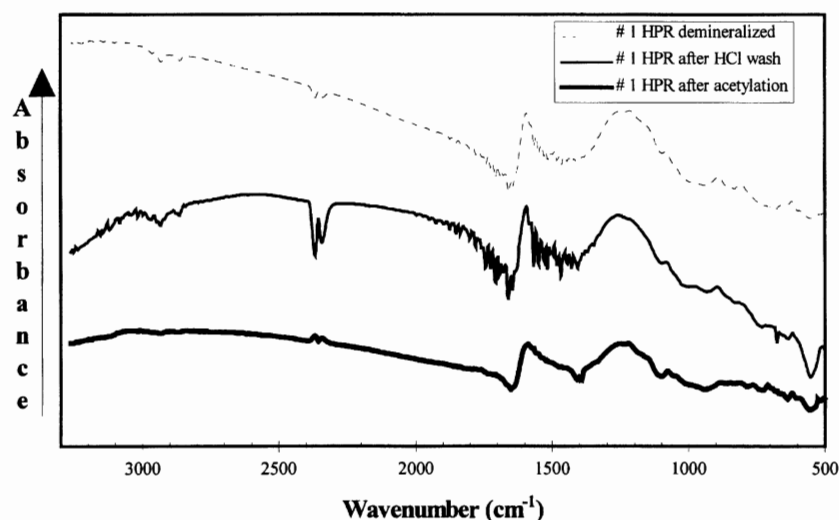


Figure 2 — FT-IR analyses did not suggest enhancement of the $1,582\text{ cm}^{-1}$ peak due to carboxylate groups. No change was observed in the IR spectra after protonation and acetylation.

Table 2 — NMR peak locations, prepared from Hatcher et al. (1985).

Peak position, ppm	Structural assignment
30	Paraffinic carbons
55	Methoxyl
72	carbohydrate or ether
106	carbohydrate (acetal)
120	aromatic (ortho or para to O substituted)
130	aromatic (unsubstituted or C-substituted)
150	aromatic (O-substituted)
175	carboxyl
190-200	Aldehyde or ketone

Department of Chemistry at the University of Utah using a CMX-100 spectroscope.

Results

FT-IR. All FT-IR spectra of demineralized SPT-floated samples of the carbonaceous material showed the presence of the $1,582\text{ cm}^{-1}$ peak from C=C stretching, as well as a broad

$1,250\text{ cm}^{-1}$ peak (Fig. 1). Several IR bands, e.g., C-O-C (stretching) and -OH (bending), are potentially responsible for the $1,250\text{ cm}^{-1}$ signal. No detectable amounts of hydrocarbons were observed in any of the samples, regardless of preg-robbing behavior. A FT-IR scan was performed on a SPT-floated head sample, before demineralization, to determine whether the acid digestion affected the spectra from the carbonaceous material. The spectra of the non-demineralized sample (Fig. 1) showed only differences from the spectra of the demineralized sample that were attributable to minerals removed during demineralization, such as carbonates ($1,435\text{ cm}^{-1}$) and silicates ($1,080\text{ cm}^{-1}$). It should be noted, however, that the CM content of the SPT-floated non-demineralized sample (~10%) is considerably lower than in the demineralized samples (41.1%). Hence, it is possible that other organic moieties are present but are not detected in the SPT-floated non-demineralized sample.

As stated above, the $1,582\text{ cm}^{-1}$ FT-IR peak activity may result from associated polar functional groups (i.e., $-\text{COO}^-$, -OH or -SH) on the aromatic ring or may result from imperfections in the structure of the aromatic matrix. Phenolic groups would have an IR signature at $1,250\text{ cm}^{-1}$ (O-H bending) and $3,400\text{ cm}^{-1}$ (O-H stretching). However, water adsorbed on the KBr would also contribute to these peaks, thereby, confounding this determination. The possible presence of phenolic and sulfhydryl groups can be investigated by acetylation (Painter et al., 1981; Starsinic et al., 1983), which forms an ester that produces an intense FT-IR band in the spectrum near $1,770\text{ cm}^{-1}$. This band appearance should, if present, be accompanied by a decrease in the $1,250\text{ cm}^{-1}$ and the $3,400\text{ cm}^{-1}$ peaks.

Likewise, the presence of carboxylate groups can be examined by submerging the sample in HCl, resulting in the protonation to carboxylic acid, which is visible in the IR spectrum near $1,720\text{ cm}^{-1}$ (Starsinic et al., 1983). Acetylation of one high preg-robbing sample (Sample #1 HPR) for 48 hrs using acetic anhydride in pyridine (Blom et al., 1957) showed no change in the FT-IR spectra (Fig. 2). None of the samples submerged in undiluted HCl showed a change in spectra, as shown in Fig. 2. Thus, it can be concluded that the $1,582\text{ cm}^{-1}$ peak is not due to the presence of phenolic, sulfhydryl or carboxyl groups associated with the aromatic rings.

The $1,250\text{ cm}^{-1}$ peak may represent a number of functionalities, including O-H stretching due to phenols and carboxylic acids, C=S stretching due to thiocarbonyls, C-H bending due to silanes (i.e., R-SiH_3), C-F₂ stretching due to fluorides and C-O-C stretching due to ether linkages. The lack of response in a and protonation experiments has ruled out the possibility that the $1,250\text{ cm}^{-1}$ peak represents phenolic and carboxylic functionalities. X-ray photoelectron spectroscopy (XPS) studies (in preparation) indicate that >90% of carbon bonds with electronegative atoms are formed with oxygen, with a minor fraction possibly formed with

Table 3 — Elemental composition of carbonaceous material. Error estimates are calculated standard deviation from multiple analysis. All values are in average weight percent.

Sample ID	O	C	As	Zn	Fe	Si	S	O/(O+C)
#1	3.68 ± 1.49	79.59 ± 4.80	1.42 ± 2.36	0.02 ± 0.03	0.16 ± 0.11	0.09 ± 0.14	5.56 ± 1.22	0.03 ± 0.02
#2	1.95 ± 0.85	85.45 ± 2.11	0.62 ± 0.91	0.03 ± 0.03	0.22 ± 0.03	0.02 ± 0.03	2.81 ± 2.55	0.02 ± 0.01
#3	2.50 ± 0.82	82.86 ± 3.15	0.13 ± 0.13	0.02 ± 0.01	0.15 ± 0.05	0.09 ± 0.14	4.77 ± 1.64	0.02 ± 0.01
#4	1.83 ± 0.84	84.47 ± 4.30	1.79 ± 2.38	0.02 ± 0.04	0.46 ± 0.78	0.03 ± 0.06	2.92 ± 1.53	0.02 ± 0.01
#5	1.96 ± 1.44	73.07 ± 7.79	8.89 ± 6.86	0.02 ± 0.02	0.39 ± 0.50	0.04 ± 0.04	5.90 ± 2.73	0.02 ± 0.01
#6	2.37 ± 1.00	83.79 ± 5.03	1.51 ± 2.51	0.03 ± 0.04	0.28 ± 0.12	0.03 ± 0.06	2.03 ± 1.47	0.02 ± 0.01
#7	2.37 ± 1.93	84.64 ± 4.61	1.41 ± 2.63	0.02 ± 0.02	0.17 ± 0.06	0.03 ± 0.04	1.70 ± 1.02	0.02 ± 0.02
HPR-1	3.43 ± 2.29	86.63 ± 4.00	1.08 ± 1.33	0.03 ± 0.04	0.05 ± 0.05	0.33 ± 0.60	1.35 ± 0.68	0.03 ± 0.02
421	3.10 ± 1.19	86.56 ± 2.06	0.17 ± 0.07	0.02 ± 0.03	0.09 ± 0.17	0.48 ± 0.87	4.43 ± 0.61	0.02 ± 0.01
418	2.72 ± 1.44	87.75 ± 4.94	1.67 ± 2.41	0.02 ± 0.02	0.05 ± 0.03	0.20 ± 0.76	2.11 ± 1.46	0.02 ± 0.02
415	2.81 ± 2.22	86.44 ± 6.21	2.65 ± 3.86	0.02 ± 0.02	0.06 ± 0.06	0.19 ± 0.56	2.26 ± 1.68	0.02 ± 0.02
11	16.77 ± 4.63	71.69 ± 6.52	0.06 ± 0.07	2.83 ± 4.40	1.21 ± 2.41	0.02 ± 0.02	0.01 ± 0.03	0.15 ± 0.04
LPR-1	12.36 ± 3.35	73.70 ± 5.94	0.05 ± 0.03	1.01 ± 1.90	0.47 ± 0.26	4.74 ± 1.93	1.17 ± 1.47	0.01 ± 0.001
# 8	5.98 ± 1.33	74.76 ± 3.63	0.06 ± 0.09	0.03 ± 0.03	0.33 ± 0.24	0.15 ± 0.21	8.34 ± 2.07	0.06 ± 0.01
# 9	2.31 ± 0.16	81.94 ± 2.35	0.60 ± 0.73	0.01 ± 0.01	0.23 ± 0.07	0.02 ± 0.01	1.32 ± 0.49	0.02 ± 0.002
0595-LPR	3.02 ± 1.44	87.01 ± 3.44	1.45 ± 2.08	0.02 ± 0.02	0.04 ± 0.03	0.02 ± 0.06	1.37 ± 0.85	0.03 ± 0.01

fluorine. Thus, it appears that the 1,250 cm⁻¹ peak is predominantly due either to thiocarbonyl or ether functionalities. Ether linkages were concluded to cause the 1,250 cm⁻¹ peak observed in Saran chars (Starsinic et al., 1983). Furthermore, the loss of oxygen during coalification towards anthracite causes dehydroxylation and formation of ethers (Tooke and Grint, 1983). The presence of oxygen substituents on the aromatic matrix, as indicated by the 1,250 cm⁻¹ peak, may also explain the asymmetry of the C=C stretch responsible for the 1,582 cm⁻¹ peak.

Electron microprobe. Minute sulfide inclusions in the CM of all samples were evident in microprobe analyses of the carbonaceous flakes (Table 3). Calculations were made to account for sulfur bound to iron, arsenic and zinc present as common minerals (pyrite, realgar and sphalerite) observed in the ore using the petrographic microscope. The mass balance indicates significant organic sulfur or unrecognized sulfides, up to 4% (by weight), may exist in the CM.

Atomic O/C ratios for the Goldstrike CM were calculated from the microprobe data using corrections for oxygen bound to silicon in quartz in cases where minute quantities of silicon were detected. No correlation was found between the O/C atomic ratio and preg-robbing characteristics (Fig. 3), which were evaluated by means of two tests: the so-called preg-robbing test, which measures loss of gold-cyanide complex (Au(CN)₂⁻) to a known amount of ore during sample batch adsorption tests, and the BTAC-CIL recovery test, which is a pilot-scale test reflecting the actual gold leaching process involving autoclaving prior to cyanidation. (These tests will be described in detail in Part 2 of this paper.) It must be noted that quantification of light elements such as oxygen and carbon with the electron microprobe is tenuous due to a poor signal-to-noise ratio for analysis of light elements by wavelength dispersive X-ray techniques. However, all O/C values are very low, as would be expected for these mature carbons.

GC-MS. Curie-point pyrolysis of methanol extracts from carbonaceous material indicated possible 0.5% to 1% humic acid and 0% to 7% fatty acids contents in the two HPR

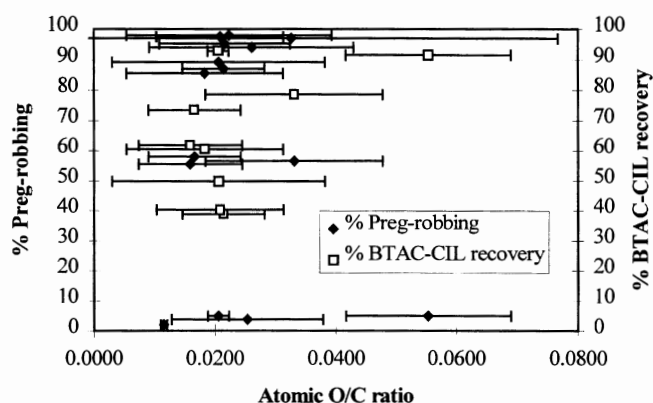


Figure 3— Plot of atomic oxygen-to-carbon ratio calculated from electron microprobe analysis vs. percent preg-robbing and percent BTAC-CIL recovery. About 15 carbonaceous particles from each sample were analyzed. Error bars denote standard deviation calculated from multiple analyses.

samples (HPR-1 and 0421) examined. Elemental sulfur contributed about 4% to 6% to the total amount of detected organic compounds, further denoting the possibility of thiocarbonyl-type structures contributing to the observed 1250 cm⁻¹ peak. Potential indicators of humic acids, such as furfural, 4-hydroxybenzaldehyde and benzoic acid were also detected. However, furfural contributes no more than 0.03% of the total mass of released organics, and 4-hydroxybenzaldehyde and benzoic acid contribute below 0.1%, indicating that the total amount of potential humic-type materials in the original sample should not exceed 0.5%. These results indicate that humic substances would not be responsible for the high preg-robbing characteristics of these two samples.

CP/MAS NMR. The low preg-robbing (LPR) sample analyzed by CP/MAS-NMR ($\delta^{13}\text{C}$) showed strong aromaticity, as did the two high preg-robbing (HPR) samples (Fig. 4). Aromatic shifts ranged from 100 to 160 ppm (Table 2). The LPR sample showed a lower signal to noise ratio due to higher conductance, presumably originating from its larger

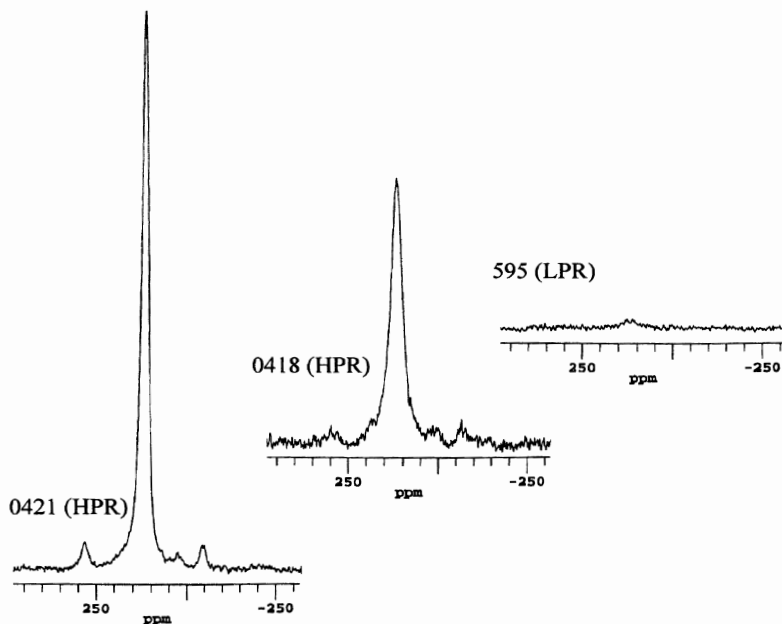


Figure 4 — $\delta^{13}\text{C}$ CP/MAS-NMR scan of samples 0595 (LPR), 0418 (HPR) and 0421 (HPR). All are shown on an equivalent intensity scale.

crystallite size. The samples showed no positive signature of aliphatic hydrocarbons. Signals from oxygenated functional groups might potentially be hidden in the shoulder of the aromatic peak at 122 ppm of the sample 0421 (HPR). However, the resolution of the analysis makes this determination impossible.

Discussion

The spectroscopic analyses in this study indicate that the carbonaceous material in the Goldstrike ore is relatively featureless, with no indication of carboxylic, phenolic or sulfhydryl functionality. The broad peak in FT-IR spectra at $1,250\text{ cm}^{-1}$ is attributable to ether or to thiocarbonyl functionalities, whereas the $1,582\text{ cm}^{-1}$ peak appears to result from either of these functionalities as substituents on the aromatic rings or from structural irregularities in the aromatic sheets comprising the carbon matrix. The FT-IR spectra of the carbonaceous matter are strikingly similar to commercial activated carbons, which have been activated at temperatures greater than 750°C (Adams, 1989).

The series of commercial activated carbons examined by Adams (1989) were heated to various temperatures under various atmospheres (N_2 , air and steam). Commercial carbons heated to temperatures less than 750°C (from 25° to 650°C) showed the presence of phenolic and carboxylic functionalities in FT-IR spectra. In contrast, carbons heated above 750°C showed only the $1,582\text{ cm}^{-1}$ peak, indicative of $\text{C}=\text{C}$ stretching, and a broad $1,250\text{ cm}^{-1}$ band, indicating possible ether functionality. Invariably, the carbons heated above 750°C showed high gold cyanide complex adsorption activities, whereas those heated to less than 750°C showed only mild gold cyanide complex uptake, and this was observed regardless of the atmosphere (N_2 , air or steam) under which heating occurred (Adams, 1989).

The similarity of the FT-IR spectra of Goldstrike ore carbonaceous material to commercial carbons activated at temperatures greater than 750°C suggest that the two are chemically equivalent. This may be surprising considering that the naturally occurring carbon in the ore presumably became activated at depth in the subsurface under anaerobic

conditions due to geologic sources of heat, whereas typical commercial activated carbons are heated under surface atmospheric conditions. However, the work of Adams (1989) shows that gold-cyanide complex uptake activity of carbon is independent of the atmosphere of activation. Instead, it depends mainly on the temperature of activation. At first glance, this may suggest that Goldstrike ore carbonaceous matter attained temperatures greater than 750°C . However, fluid inclusion studies of methane from Carlin ore carbonaceous material and of CO_2 and H_2O in quartz minerals suggest that the maximum temperatures achieved during organic-matter maturation and mineralization ranged from 135° to 300°C under 0.6 to 1.4 kbars pressure (Kuehn and Rose, 1995).

The expectation of similar maturation temperatures between natural carbonaceous matter and commercial activated carbon on the basis of similar chemistries may be naive, given the vast differences in their respective maturation times, i.e.,

maturation over geologic vs. industrial processing-time scales. One can speculate that maturation over long periods at relatively low temperatures might produce the same carbon as maturation at relatively high temperatures over relatively short periods.

To out compete commercial carbon for aurocyanide, the naturally occurring ore carbon may not necessarily need to have as high a gold-cyanide complex uptake capacity. The kinetics of gold-cyanide complex sorption to the relatively fine-grained naturally occurring ore carbonaceous material may be faster than uptake kinetics of the coarser-grained commercial activated carbon. This would allow greater gold-cyanide complex uptake by the natural ore carbonaceous material over the time-scale of ore processing, despite a possible greater equilibrium gold-cyanide complex uptake capacity by the commercial carbon.

Hausen and Bucknam (1985) showed that the kinetics of gold-cyanide complex uptake by Carlin ore carbonaceous material were four times faster than the uptake kinetics of commercial activated carbon, whereas the equilibrium gold-cyanide complex uptake capacity by commercial activated carbon was ten times greater relative to Carlin ore carbonaceous material.

The results of this study appear to indicate that naturally occurring carbonaceous material in the Goldstrike ore takes up aurocyanide by the same mechanism as the commercial activated carbon that is introduced later in the plant process. However, it is possible that other analyses will distinguish the mechanisms of aurocyanide association with these carbons.

Future studies will examine the kinetics and equilibria of aurocyanide adsorption to, and desorption from, high and low preg-robbing natural carbonaceous matter and commercial activated carbon, with the objective of distinguishing the mechanisms of aurocyanide association with these materials.

Conclusions

No detectable amounts of humic substances or hydrocarbons were found in either high or low preg-robbing carbonaceous material from BGMI. Based on the analyses per-

formed in this study, it is believed that the carbonaceous material from the Goldstrike Mines consists of relatively featureless aromatic structures forming an activated carbon or graphite-type matrix with ether or thiocarbonyl functionality. This is in agreement with earlier studies of Carlin trend carbonaceous material (Nelson et al., 1982; Leventhal and Hofstra, 1990; Sibrell et al., 1990) and other studies of mature activated carbon (Adams, 1989) and coal (Starsinic et al., 1983). Similarity of the FT-IR spectra of Goldstrike ore carbonaceous material and commercial activated carbon heated above 750°C suggests chemical equivalence of these carbons.

The presence of ether or thiocarbonyl functionalities is indicated by FT-IR analyses. But this determination requires further analyses. Microprobe analyses showed that minute sulfide inclusions are present in the CM along with potential organic sulfur. Atomic oxygen to carbon ratios did not show a correlation with respect to preg-robbing characteristics. However, the atomic oxygen to carbon ratios did show that the organic carbon is of high maturity, equal to or higher than anthracite grade coal.

Acknowledgements

The authors wish to acknowledge and thank Barrick Goldstrike Mines Inc. for providing funding for this project. The authors would also like to acknowledge the staff at Barrick Goldstrike Metallurgical Services for collecting samples and providing metallurgical and LECO analyses. Thanks also go Dr. Bill Parry, Department of Geology and Geophysics, University of Utah; Philip L. Sibrell for his helpful advice throughout the project; Dr. Erich U. Petersen, Department of Geology and Geophysics, University of Utah, for providing assistance with microprobe analysis; Dr. Jan Miller, Department of Metallurgical Engineering, University of Utah, for access to the FT-IR; Dr. Saskia Duyvesteyn, Department of Metallurgical Engineering, University of Utah, for advice and corrections; Jacek P. Dworzanski, Center for Micro Analysis and Reaction Chemistry, University of Utah, for assisting with interpretation of GC-MS results; and Yongqiang Lu, Department of Metallurgical Engineering, University of Utah, for assistance with the FT-IR.

References

Adams, M.D., 1989, Ph.D. Dissertation, University of the Witwatersrand, Johannesburg, South Africa, 387 pp.

Blom, L., Edelhausen, L., and Van Krevelen, D.W., 1957, "Chemical structures and properties of coal CVII - oxygen groups in coal and related products," *Fuel*, Vol. 36, pp. 135-153.

Hatcher, P.G., Spiker, E., and Orem, W.H., 1985, "Oxidative origin of sedimentary humic acids, important carriers of metals," *Organics and Ore Deposits*, W.E. Dean, ed., Denver Region Exploration Geologists Society, Wheat Ridge, CO, pp. 57-66.

Hausen, D.M., and Bucknam, C.H., 1985, "Study of preg-robbing in the cyanidation of carbonaceous gold ores from Carlin, Nevada," *Applied Mineralogy, Proceedings of the Second International Congress on Applied Mineralogy*, W.C. Park, D.M. Hausen, and R.D. Hagni, eds., AIME, Warrendale, PA, pp. 833-856.

Hausen, D.M., and Park, W.C., 1985, "Observations on the association of gold mineralization with organic matter in Carlin-type ores," *Organics and Ore Deposits*, W.E. Dean, ed., Denver Region Exploration Geologists Society, Wheat Ridge, CO, pp. 119-136.

Kuehn, C.A., and Rose, A.W., 1995, "Carlin gold deposits, Nevada: Origin in a deep zone of mixing between normally pressured and overpressured fluids," *Economic Geology*, Vol. 90, pp. 17-36.

Leventhal, J.S., 1985, "Roles of organic matter in ore deposits," *Organics and Ore Deposits*, W.E. Dean, ed., Denver Region Exploration Geologists Society, Wheat Ridge, CO, pp. 7-20.

Leventhal, J.S., and Hofstra, A., 1990, "Characterization of carbon in sediment-hosted disseminated gold deposits, north-central, Nevada," *Gold '90*, SME Symposium, Salt Lake City, UT, pp. 365-368.

Mantell, C.L., 1968, *Carbon and Graphite Handbook*, Interscience Publishers, New York, pp. 8-21.

Miller, J.D., and Sibrell, P.L., 1991, "The nature of gold adsorption from cyanide solutions by carbon," *EPD Congress '91*, The Minerals, Metals & Materials Society, Warrendale, PA, pp. 647-663.

Nakamizo, M., Honda, H., and Inagaki, M., 1978, "Raman spectra of ground natural graphite," *Carbon*, Vol. 16, No. 4, pp. 281-283.

Nelson, J.H., MacDougall J.J., Baglin, F.G., Freeman D.W., Nadler, M., and Hendrix, J.L., 1982, "Characterization of Carlin-type gold ore by photoacoustic, Raman and EPS spectroscopy," *Applied Spectroscopy*, Vol. 36, pp. 574-576.

Painter, P.C., Snyder, R.W., Starsinic, M., Coleman, M.M., Kuehn, D.W., and Davis, A., 1981, "Concerning the application of FT-IR to the study of coal: A critical assessment of band assignments and the application of spectral analysis programs," *Applied Spectroscopy*, Vol. 35, No. 5, pp. 475-485.

Painter, P.C., Starsinic, M., Squires, E., and Davis, A.A., 1983, "Concerning the 1600 cm⁻¹ region in the i.r. spectrum of coal," *Fuel*, Vol. 62, pp. 742-744.

Radtke, A.S., and Scheiner, B.J., 1970, "Studies of hydrothermal gold deposition (I). Carlin gold deposits, Nevada: The role of carbonaceous materials in gold deposition," *Economic Geology*, Vol. 65, pp. 87-102.

Sibrell, P.L., Wan, R.Y., and Miller, J.D., 1990, "Spectroscopic analysis of passivation reactions for carbonaceous matter from Carlin trend ores," *Gold '90*, SME symposium, Salt Lake City, UT, pp. 355-363.

Sibrell, P.L., 1991, "The characterization and treatment of Carlin trend carbonaceous gold ores," Ph.D. Dissertation, University of Utah, Salt Lake City, 196 pp.

Sibrell, P.L., and Miller, J.D., 1992, "Significance of graphitic structural features in gold adsorption by carbon," *Minerals and Metallurgical Processing*, pp. 189-195.

Smith, G.C., 1968, "Discussion of refractory ore," Carlin Gold Mining Company, Feb. 20, unpublished report.

Snyder, R.W., Painter, P.C., Havens, J.R., and Koenig, J.L., 1983, "The determination of hydroxyl groups in coal by Fourier Transform Infrared and ¹³C NMR spectroscopy," *Applied Spectroscopy*, Vol. 37, No. 6, pp. 497-502.

Sobkowiak, M., and Painter, P., 1992, "Determination of the aliphatic and aromatic CH contents of coals by FT-IR: Studies of coal extracts," *Fuel*, Vol. 71, pp. 1105-1125.

Starsinic, M., Rodney, L.T., Walker, P.L. Jr., and Painter, P.C., 1983, "FT-IR studies of Saran chars," *Carbon*, Vol. 21, No. 1, pp. 69-74.

Stenebråten, J.F., Johnson, W.P., and McMullen, J., (to be published), "Characterization of Goldstrike ore carbonaceous matter, Part 2: Physical characteristics," *Minerals & Metallurgical Processing*.

Tafari, W.J., 1987, "Geology and geochemistry of the Mercur district, Utah," Ph.D. Dissertation, University of Utah, Salt Lake City, pp. 126-127.

Tooke, P.B., and Grint, A., 1983, "Fourier transform infrared studies of coal," *Fuel*, Vol. 63, pp. 1003-1008.

Tuinstra, F., and Koenig, J.L., 1970, "Raman spectrum of graphite," *The Journal of Chemical Physics*, Vol. 53, No. 3, pp. 1126-1130.

Zerda, T.W., Andrzej, J. and Chmura, K. 1981, "Raman studies of coal," *Fuel*, Vol. 60, pp. 375-378.